Hysteresis and bi-stability in a realistic cell-model for calcium oscillations and action potential firing

J.M.A.M. Kusters,[1] J.M. Cortes,[1,2] W.P.M. van Meerwijk,[3] D.L.Ypey,[3] A.P.R. Theuvenet,[3] and C.C.A.M. Gielen[1]

[1] *Dept. of Biophysics, Radboud University Nijmegen, 6525 EZ Nijmegen, The Netherlands*
[2] *Institute for Adaptive and Neural Computation. School of Informatics, University of Edinburgh, EH1 2QL, UK*
[3] *Dept. of Cell Biology, Radboud University Nijmegen, 6525 ED Nijmegen, The Netherlands*

(Dated: October 25, 2006)

Many cells reveal oscillatory behavior. Some cells reveal action potential firing corresponding to Hodgkin-Huxley (HH) type dynamics of ion-channels in the cell membrane. Another type of oscillation relates to periodic IP3-mediated calcium transients in the cytosol. In this study we present a bifurcation analysis of a cell with an excitable membrane and an IP_3-mediated intracellular calcium oscillator. With IP_3 concentration as a control parameter the model reveals a complex, rich spectrum of both stable and unstable solutions with hysteresis corresponding to experimental data. The range of hysteresis is largest for realistic parameter values of the model, illustrating the functional importance of hysteresis.

PACS numbers: 05.45.-a ; 05.70.Ln ; 87.16.Ac ; 89.20.-a

Complexity and transitions among stable and unstable states are ubiquitous in biological systems [1, 2]. In physics instabilities in emerging collective properties have been studied since many years [3–6]. Recently the phenomenon of multi-stability with hysteresis has also awakened a large interest in biology [7]. Instabilities, for instance, have been shown to be responsible for genetic alterations in tumor development[8, 9] and for efficient information processing in the brain, such as in odor encoding [10, 11]. Multistable systems allow changes among different stable states. These transitions can be due to external input or due to instabilities which may serve as an alternative to switch between different branches of stable states [7]. Bistability is advantageous to prevent the system from reaching intermediate states. In addition, hysteresis may help to keep the system in a particular stable state, preventing it from sliding back to another state [12]. This is useful, for instance, in cell mitosis. Once initiated, it should not be terminated before completion [13].

At the network level, multistability plays an important role in cell signaling as well [14, 15]. Communication between cells takes place at synaptic contacts, where an action potential arrival releases a neurotransmitter, thus affecting the post-synaptic potential of the target cell. This information at the cell membrane is transferred to the cell nucleus by second messengers, causing gene expression. Calcium is one such second messenger and calcium transients have been observed over a wide range of frequencies, with a chaotic or deterministic oscillating pattern [16].

Oscillatory behavior of cells is typically the result of two mechanisms. The first mechanism is located at the cell membrane and is related to periodic action-potential firing, usually triggered by input from other cells in the network. The other mechanism relates to oscillations in the concentration of free intracellular calcium by calcium release from the endoplasmic reticulum (ER) store. In this study we show how coupling of these two simple systems leads to a rich behavior with multiple stable and unstable states with hysteresis, in agreement with experimental observations. We present a simplified model, which captures the basic characteristics of normal rat kidney (NRK) fibroblasts reported in [17], and which reproduces, on the basis of single-cell and single-channel data [18], the kinetics for both the membrane ionic currents and the intracellular calcium oscillator.

The dynamics of the NRK membrane potential depends on the sum of ion currents through the membrane:

$$\frac{dV_m}{dt} = -\frac{1}{C_m}\sum_i I_i \tag{1}$$

where V_m is the membrane potential and C_m=20 pF is the capacitance of the membrane. The most relevant currents are those through the inward rectifier potassium channel (I_{Kir}), the L-type Ca-channels (I_{CaL}), Ca-dependent chloride channels ($I_{Cl(Ca)}$), leak channels (I_{lk}), and SOC-channel (I_{SOC}). The dynamics of the L-type Ca-channel is given by $I_{CaL} = m\,h\,G_{CaL}\,(V_m - E_{CaL})$ with an activation (m) and inactivation (h) variable. The dynamics of m and h are described by first order differential equations of the type

$$\frac{dx}{dt} = \frac{x_\infty(V) - x}{\tau_x(V)} \tag{2}$$

where x_∞ and τ_x correspond to the steady-state (membrane potential and conductance-dependent) (in)activation and time constant, respectively.

The Ca-dependent Cl-current $I_{Cl(Ca)}$ is given by

$$I_{Cl(Ca)} = \frac{[Ca^{2+}_{cyt}]}{[Ca^{2+}_{cyt}]+K_{Cl(Ca)}}\,G_{Cl(Ca)}\,(V_m - E_{Cl(Ca)}). \tag{3}$$

The Cl-current increases with cytosolic calcium concentration $[Ca^{2+}_{cyt}]$, causing a depolarization to the Nernst

potential of Cl ions $E_{Cl(Ca)}$ near -20 mV. For the definition of the other currents, see [19]; for details, see [17].

The flux of calcium through the membrane is the sum of the fluxes of Ca^{2+} ions through the L-type Ca-channel and the SOC-channel and by extrusion by the PMCA-pump $J_{PM} = -\frac{1}{z_{Ca}FA_{PM}}(I_{CaL} + I_{SOC}) - J_{PMCA}$.

Calcium in the cytosol is buffered by proteins in the cytosol. Buffering is described by first order interactions between $[Ca^{2+}_{cyt}]$ and the concentration of the buffer

$$\frac{d[BCa]}{dt} = k_{on}([T_B] - [BCa])[Ca^{2+}_{cyt}] - k_{off}[BCa] \quad (4)$$

where $[T_B]$ represents the total buffer concentration and $[BCa]$ represents the concentration of buffered calcium.

The dynamics for the calcium concentration in the ER depends on the sum of fluxes through the IP3-receptor (J_{IP_3R}), leak through the ER-membrane (J_{lkER}) and by (re)uptake by the SERCA pump (J_{SERCA})

$$\frac{d[Ca^{2+}_{ER}]}{dt} = \frac{A_{ER}}{Vol_{ER}}(-J_{IP_3R} - J_{lkER} + J_{SERCA}) \quad (5)$$

where the ratio of the surface A_{ER} and the volume Vol_{ER} of the ER transforms the flux of Ca^{2+}-ions through the ER-membrane into changes of Ca^{2+}_{ER}-concentration. The flux through the IP_3-receptor is described by

$$J_{IP_3R} = f_\infty^3 \, w^3 \, K_{IP_3R} \, ([Ca^{2+}_{ER}] - [Ca^{2+}_{cyt}]) \quad (6)$$

where $[Ca^{2+}_{ER}] - [Ca^{2+}_{cyt}]$ is the concentration difference between calcium in the ER and in the cytosol. K_{IP_3R} is the rate constant per unit area of IP_3-receptor mediated release. f_∞ and w represent the fraction of open activation and inactivation gates, respectively. The dynamics of f and w is given by Eq. 2, but since the time constant for f is fast, we use f_∞ instead of f. f_∞ and w_∞ depend both on the cytosolic calcium concentration :

$$f_\infty = \frac{[Ca^{2+}_{cyt}]}{K_{fIP_3} + [Ca^{2+}_{cyt}]} \quad (7)$$

$$w_\infty = \frac{\frac{[IP_3]}{K_{wIP_3}+[IP_3]}}{\frac{[IP_3]}{K_{wIP_3}+[IP_3]} + K_{w(Ca)}[Ca^{2+}_{cyt}]} \quad (8)$$

The excitable membrane and the IP3-oscillator are coupled by $[Ca^{2+}_{cyt}]$. During an action potential opening of the L-type calcium channel causes a large inward current of Ca-ions in the plasma membrane. The increased $[Ca^{2+}_{cyt}]$ activates the IP_3-receptor by increasing f_∞ (Eq. 7), causing an intracellular calcium transient. In the opposite process, IP_3-mediated calcium oscillations cause periodic calcium transients, which open the Ca-dependent Cl-channels (Eq. 3). The depolarization of the membrane towards the Nernst potential near -20 mV causes activation of the L-type Ca-channels in the plasma membrane. After an action potential or Ca-oscillation the reduction of cytosolic calcium by the activity of the SERCA and PMCA pump reduces $I_{Cl(Ca)}$, such that the membrane repolarizes to the rest potential near - 70 mV.

The dynamics of the complete single-cell model depends on the time evolution of the 7-dimensional vector $\vec{x}(t) = (m, h, w, [BCa], V_m, [Ca^{2+}_{cyt}], [Ca^{2+}_{ER}])^T$. Using Eqs. 1, 2, 4 and 5 and keeping in mind the dependence of $[Ca^{2+}_{cyt}]$ on the Ca-fluxes through cell membrane and ER-membrane, this can be written as

$$\dot{\vec{x}}(t) = \vec{f}(\vec{x}(t)) \quad (9)$$

In order to find the stable states of $\vec{x}(t)$ it is important to notice that the cell behavior corresponds to an autonomous nonlinear dynamical system with periodic oscillatory behavior. To find its stable periodic solutions we assume that $\tilde{\vec{x}}(t)$ is the periodic solution of the system in Eq. 9. For any perturbation $\vec{y}(t)$ around the stable periodic solution $\tilde{\vec{x}}(t)$ substitution of the solution $\vec{x}(t) = \tilde{\vec{x}}(t) + \vec{y}(t)$, Taylor expansion around the period solution $\tilde{\vec{x}}(t)$ and retaining only linear terms, gives

$$\dot{\vec{y}}(t) = J(\vec{x}(t))\vec{y}(t) \quad (10)$$

where $J(\vec{x}(t))$ is the Jacobian matrix $\nabla_{\vec{x}} f(\vec{x}(t))$ at the point $\vec{x}(t)$ on the periodic solution. The eigenvectors $\vec{y}_i(t)$ of J form the fundamental matrix $\Phi(t) = [\vec{y}_1(t), \vec{y}_2(t), ..., \vec{y}_n(t)]$. Any fundamental solution to the matrix of the T-periodic system in Eq. 10 can be written in the form $Y(t) = Z(t)e^{t\Phi}$, where Y, Z and Φ are nxn matrices ([20]) with $Z(t) = Z(t+T)$. In particular we can choose $Y(0) = Z(0) = I$, so that $Y(T) = Z(T)e^{T\Phi} = Z(0)e^{T\Phi}$. It then follows that the behavior of the solutions in the neighborhood of $\tilde{\vec{x}}(t)$ is determined by the eigenvalues of the matrix $e^{T\Phi}$. The (complex) eigenvalues λ_i of this matrix (the Floquet multipliers ([20])) provide a measure of the local orbital divergence ($|\lambda_i| > 1$) or convergence ($|\lambda_i| < 1$) along a particular direction over one period of the periodic motion.

We will explore the bifurcation behavior and local stability of the electrically excitable membrane and intracellular calcium oscillator, separately, and then compare the results for a complete model, where the membrane oscillator and intracellular calcium oscillator are coupled, using the software packages *AUTO* [21] and *XPP* [21].

The excitable membrane can be studied in isolation by setting the IP_3 concentration to zero to eliminate persistent intracellular calcium oscillations. The dynamics of the membrane is studied as a function of the leakage parameter K_{lkER} to produce variations in $[Ca^{2+}_{cyt}]$. Fig. 1 shows the hysteresis diagram for the membrane with the steady states of $[Ca^{2+}_{cyt}]$ (A) and the membrane potential V_m (B). $[Ca^{2+}_{cyt}]$ and V_m increase gradually until $K_{lkER} \approx 58.0 \times 10^{-8} dm/s$. Then the increased calcium concentration opens the $Cl(Ca)$-channels and

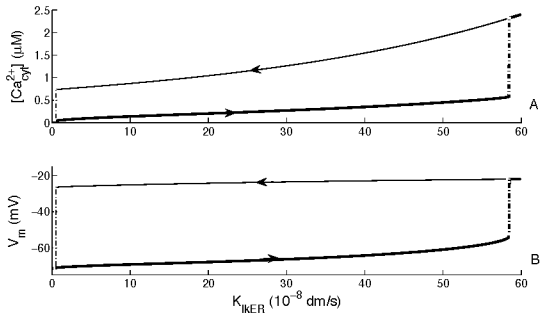

FIG. 1: Hysteresis diagram for the excitable membrane with K_{lkER} as a control parameter for the stable steady solutions for the calcium concentration in the cytosol (A) and membrane potential (B). Arrows show the direction of evolution of the system for increasing and decreasing values of K_{lkER}.

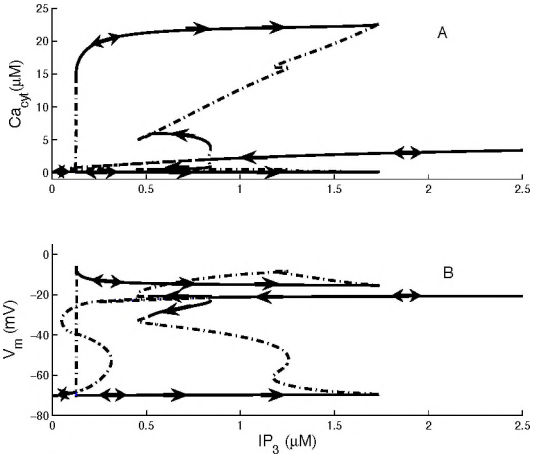

FIG. 2: Bifurcation diagram for the complete cell model with the cytosol calcium concentration (A) and membrane potential (B) as a function of IP_3. Solid and dashed lines correspond to stable and unstable states, respectively. Arrows show the direction of evolution of the system for increasing and decreasing IP_3 values.

the membrane potential depolarizes to the Nernst potential of the $Cl(Ca)$-channels close to $-20\ mV$ (see Fig. $1B$). This sudden depolarisation opens the $L-$type Ca-channels causing a calcium inflow through the membrane into the cytosol, which explains the sudden increase of $[Ca^{2+}_{cyt}]$ until 2.3 μM. When K_{lkER} is decreased, the $L-$type Ca-channels are open, causing an increased $[Ca^{2+}_{cyt}]$. This explains why the $Cl(Ca)$-channels are open and why the membrane potential remains near -20 mV. Only when $[Ca^{2+}_{cyt}]$ decreases to low concentrations, the $Cl(Ca)$-channels close and the membrane potential repolarizes to $-70\ mV$.

The dynamics of the intracellular calcium oscillator as a function of the IP_3 concentration can be studied by blocking the $L-$type $Ca-$channels (G_{CaL}=0). The bifurcation diagram shows a stable state at low IP3-concentrations, followed by a subcritical Hopf-bifurcation, where the IP3-receptor shows periodic oscillations (open/closed) and large calcium transients in the cytosol. The oscillation frequency increases with IP3-concentration until a subcritical Hopf bifurcation brings the system into a stable state where the IP3-receptor is continuously open with a constant leak of calcium into the cytosol, see [22, 23]. The bifurcation diagram looks very similar to the top panel in Fig. 3.

The bifurcation diagram for the complete single-cell model is illustrated in Fig. 2, which shows cytosolic calcium concentration (A) and membrane potential (B) as a function of IP_3. The solid and dashed lines represent stable and unstable states, respectively. For small IP_3 values the cell has a single stable steady state. For $IP_3 > 0.15\ \mu M$ the stable fixed point becomes unstable in a subcritical Hopf bifurcation. Calcium oscillations with action potentials (B) occur for $IP_3 \in (0.15, 1.75)$ μM. In this regime, a rapid calcium inflow from the ER into the cytosol opens the $Ca(Cl)-$channel, causing an inward current towards the $Cl-$Nernst potential at $-20\ mV$. After closure of the IP_3-receptor, calcium is removed from the cytosol by Ca-pumps in the cell membrane and ER, leading to repolarisation to -70 mV. For $IP_3 > 1.75\ \mu M$, the fixed point $(Ca_{cyt}, V_m) \approx (3.00\ \mu M, -20\ mV)$ becomes stable in a subcritical Hopf bifurcation. When IP_3 is high, the IP_3-receptor acts as a constant leak of calcium into the cytosol which opens the $Ca(Cl)$-channels, causing a depolarization to the Cl-Nernst potential near $-20\ mV$ (B).

If IP_3 decreases, the cell reveals a complex hysteresis pattern. For decreasing IP_3 concentrations, the system stays in a single stable steady state with an elevated Ca_{cyt} near 3 μM and a membrane potential near -20 mV until $IP_3 \approx 0.85\ \mu M$. Then, crossing through a Hopf bifurcation causes instability (dashed line) forcing the system to behave as a stable oscillator with calcium oscillations (amplitude $\approx 6\ \mu$M) and small membrane potential oscillations around $-20\ mV$. These oscillations are due to interaction between the L-type Ca-channel and the $IP3$-receptor at elevated cytosolic calcium concentrations. At $IP_3 \approx 0.45\ \mu M$ the stable oscillator becomes unstable (dashed line), returning the system to the stable oscillations with large Ca-transients and action potentials. Finally, for IP_3 values smaller than 0.15 μM the system returns to a single stable state.

Since the SOC channel in the plasma membrane plays a crucial role in stabilization of the calcium dynamics [17], we studied the dynamics of the cell as a function of the conductance of the SOC channel. Figure 3 shows the hysteresis diagrams for increasing values of G_{SOC}. As explained in [17], the cell behavior is unstable for $G_{SOC} = 0.00\ nS$ with either depletion or accumulation of calcium in the ER. For small values of G_{SOC} bista-

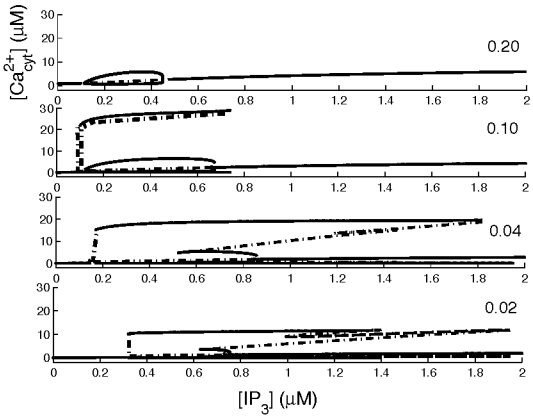

FIG. 3: Bifurcation diagrams for different values of G_{SOC}. Variations in $[Ca^{2+}_{cyt}]$are due to both $IP3$-mediated calcium oscillations and action potentials for all G_{SOC}-values except for $G_{SOC} = 0.20\ nS$, where the action potentials disappear. For values of G_{SOC} near $0.04\ nS$ the $IP3$-range of hysteresis has a maximum.

bility and hysteresis appears. The range of IP3-values with hysteresis is largest for G_{SOC} near $0.04\ nS$ (see Fig. 3). For higher values of G_{SOC}, the range of hysteresis decreases until only the typical Hopf-bifurcation for the IP3-mediated calcium oscillations remains for $G_{SOC} = 0.20\ nS$.

The SOC conductance, which gives the largest hysteresis loop, corresponds to the observed SOC-conductance in the literature ([24] and [25] with values in the range from 0.04 to 0.05 nS. For hepatocytes SOC conductances are between $(0.08, 0.14)\ nS$ [26] , but taking into account that the density of ionic channels in hepatocytes is twice as high as in fibroblasts [27, 28], the range of SOC-conductances which produce the largest amount of hysteresis is in agreement with values reported by [24, 25] and with our simulation results.

Summarizing, we have presented a model reproducing experimental data on calcium oscillations and action potential generation. A bifurcation analysis reveals hysteresis and a complex spectrum of stable and instable states. Stability of the cell behavior is dominated by the homeostatic function of the SOC channel. The conductance, which provides the largest range of hysteresis, coincides with the measured values for G_{SOC}.

We acknowledge support from the Netherlands Organisation for Scientific Research, Ministerio de Educacion y Ciencia, Junta de Andalucia and Eng. and Physical Sciences Research Council, grants NWO 805.47.066, MEC FIS2005-00791, JA FQM-165, EPSRC EP/C0 10841/1.

[1] J. D. Murray, *Mathematical Biology I. An Introducion* (Springer, 2002).

[2] H. Kitano, ed., *Foundations of Systems Biology* (MIT, 2001).

[3] H. Haken, Rev Mod Phys **47**, 67 (1975).

[4] B. J. T. Jones, Rev Mod Phys **48**, 107 (1976).

[5] C. Normand, Y. Pomeau, and M. G. Velarde, Rev Mod Phys **49**, 581 (1977).

[6] M. C. Cross and P. C. Hohenberg, Rev Mod Phys **65**, 851 (1993).

[7] P. Ashwin and M. Timme, Nature **436**, 36 (2005).

[8] C. Lengauer, K. W. Kinzler, and B. Vogelstein, Nature **17**, 643 (1998).

[9] R. Gryfe, H. Kim, E. T. K. Hsieh, M. D. Aronson, E. J. Holowaty, S. B. Bull, M. Redston, and S. Gallinger, N Engl J Med **342**, 69 (2000).

[10] M. Rabinovich, A. Volkovskii, P. Lecanda, R. Huerta, H. D. Abarbanel, and G. Laurent, Phys Rev Lett **87**, 068102 (2001).

[11] G. Laurent, M. S. R. W. Friedrich, M. I. Rabinovich, A. Volkovskii, and H. D. Abarbanel, Annu Rev Neurosci **24**, 263 (2001).

[12] M. J. Solomon, Proc Natl Acad Sci USA **100**, 771 (2003).

[13] W. Sha, J. Moore, K. Chen, A. Lassaletta, C. S. Yi, J. J. Tyson, and J. C. Sible, 2003 **100**, 975 (Proc Natl Acad Sci USA).

[14] M. Laurent and N. Kellershohn, Trends Biochem Sci **24**, 418 (1999).

[15] D. Angeli, J. E. Ferrell, and E. D. Sontag, Proc Natl Acad Sci USA **101**, 1822 (2004).

[16] T. R. Chay and J. Rinzel, Biophys J **47**, 357 (1985).

[17] J. M. A. M. Kusters, M. M. Dernison, W. P. M. van Meerwijk, D. L. Ypey, A. P. R. Theuvenet, and C. C. A. M. Gielen, Biophys J **89**, 3741 (2005).

[18] E. G. Harks, J. J. Torres, L. N. Cornelisse, D. L. Ypey, and A. P. Theuvenet, J Cell Physiol **196**, 493 (2003).

[19] *The leak current is defined by* $I_{lk} = G_{lk}\ (V_m - E_{lk})$. *The current through the soc-channel is given by* $I_{SOC} = \frac{K_{SOC}}{[Ca^{2+}_{cyt}]+K_{SOC}} G_{SOC}\ (V_m - E_{SOC})$. *This current increases when the concentration of calcium in the ER decreases and plays an important role in calcium homeostasis of the cell.*

[20] J. Guckenheimer and P. Holmes, *Nonlinear Oscillations, Dynamical Systems, and Bifurcations of Vector Fields*, vol. 42 (Springer Verlag, 1983).

[21] T. F. Fairgrieve and A. D. Jepson, SIAM Journal on Numerical Analysis **28**, 1446 (1991).

[22] S. Schuster, M. Marhl, and T. Hofer, Eur J Biochem **269**, 1333 (2002).

[23] Y. Li and J. Rinzel, J Theor Biol **166**, 461 (2002).

[24] A. B. Parekh and J. W. Putney, Physiol Rev **85**, 757 (2005).

[25] E. Krause, F. Pfeiffer, A. Schmid, and I. Schulz, J Biol Chem **271**, 32523 (1996).

[26] G. Y. Rychkov, T. Litjens, M. L. Roberts, and G. J. Barritt, Cell Calcium **37**, 183 (2005).

[27] A. D. G. D. Roos, Ph.D. thesis, Katholieke Universiteit Nijmegen, The Netherlands (1997).

[28] Z. Yin and M. Watsky, Am J Physiol Lung Cell Mol Physiol **288**, L1110 (2005).